



## Accepted Article

**Title:** Geometries of 11-vertex carborane monoanion radicals with  $2n+3$  skeletal electron counts

**Authors:** Mark A. Fox, Natasha C. D. Patel, and Josep M. Oliva-Enrich

This manuscript has been accepted after peer review and appears as an Accepted Article online prior to editing, proofing, and formal publication of the final Version of Record (VoR). This work is currently citable by using the Digital Object Identifier (DOI) given below. The VoR will be published online in Early View as soon as possible and may be different to this Accepted Article as a result of editing. Readers should obtain the VoR from the journal website shown below when it is published to ensure accuracy of information. The authors are responsible for the content of this Accepted Article.

**To be cited as:** *Eur. J. Inorg. Chem.* 10.1002/ejic.201700419

**Link to VoR:** <http://dx.doi.org/10.1002/ejic.201700419>

# Geometries of 11-vertex carborane monoanion radicals with $2n+3$ skeletal electron counts.

Natasha C.D. Patel,<sup>a</sup> Josep M. Oliva-Enrich<sup>b,\*</sup> and Mark A. Fox<sup>a,\*</sup>

<sup>a</sup>Department of Chemistry, Durham University, Durham DH1 3LE, United Kingdom.

E-mail: m.a.fox@durham.ac.uk

<http://www.dur.ac.uk/chemistry/staff/profile/?id=182>

<sup>b</sup>Institute of Physical Chemistry “Rocasolano”, CSIC, Serrano 119, 28006 Madrid, Spain.

E-mail: j.m.oliva@iqfr.csic.es

<https://energymass.iqfr.csic.es/home-4/josep-m-oliva>

*Supporting Information:* Additional computational data including conformers of **5** and simulated EPR spectra for 11-vertex radicals [3-5]<sup>+</sup>.

## Keywords

Carboranes; Skeletal electrons; Clusters; Cyclic voltammetry; Electron paramagnetic resonance

For “Boron Chemistry – A Rapidly Expanding Field”

Special Issue - *Eur. J. Inorg. Chem.*

## Abstract

While geometries of 12- and 13-vertex dicarbaborane (carborane) radicals with rare  $2n+3$  skeletal electrons have been determined elsewhere, the geometries of the 11-vertex dicarbaborane monoanion radicals with  $2n+3$  SE are established here for the first time by computations in agreement with observed electrochemical and electron paramagnetic resonance spectroscopy (EPR) data.

## Introduction

Carborane clusters are generally governed by the skeletal electron-counting rules with closed clusters containing  $2n+2$  skeletal electrons (SE) and open clusters containing  $2n+4$  SE.<sup>[1,2]</sup> Both  $2n+2$  SE and  $2n+4$  clusters, usually classed as *closo* and *nido* clusters respectively, are



monoanion radical and between the monoanion radical and the dianion in CV measurements. On this basis, the most stable 12-vertex  $2n+3$  radical reported so far is  $[2]^{\bullet-}$  from reduction of the 1,2-diaryl-*ortho*-carborane **2** where the aryl group is the electron-withdrawing 4-trifluoromethyltetrafluorophenyl unit (Figure 2).<sup>[19]</sup>

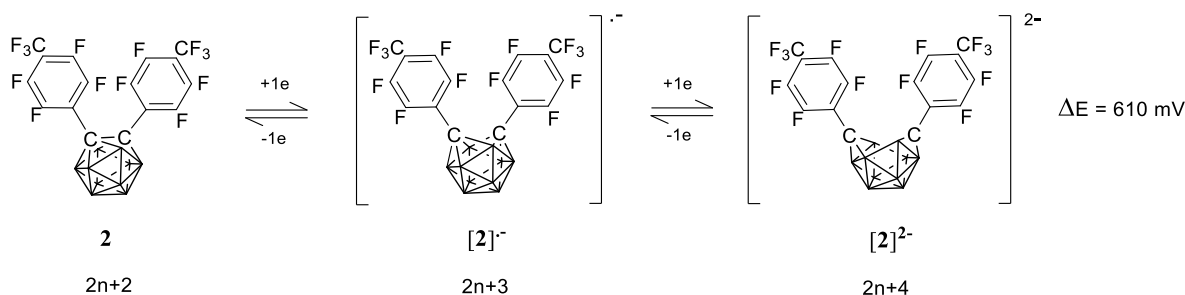


**Figure 2.** Two one-electron reductions for 1,2-bis(4'-trifluoromethyltetrafluorophenyl)-*ortho*-carborane **2**.

A stable  $2n+3$  radical was isolated as a salt in 2007 by chemical reduction of a 13-vertex carborane derivative.<sup>[21]</sup> The geometry of this salt was determined by X-ray crystallography and is slightly more open than the geometry corresponding to the  $2n+2$  13-vertex cluster. More 13-vertex  $2n+3$  dicarbaborane radicals were isolated recently and such clusters were examined computationally to determine why 13-vertex  $2n+3$  radicals are more stable than 12- and 14-vertex  $2n+3$  radicals.<sup>[22]</sup>

A less well-known class of  $2n+3$  radicals from chemical and electrochemical reductions of 11-vertex dicarbaboranes **3-6** was published in a 1975 study (Figure 3).<sup>[23]</sup> The  $2n+2$  compound, 2,3-(CH<sub>3</sub>)<sub>2</sub>-2,3-C<sub>2</sub>B<sub>9</sub>H<sub>9</sub> **3**, gave an unstable  $2n+3$  radical  $[3]^{\bullet-}$  on reduction but the three derivatives **4-6** with bridges attached to borons 4 and 7 resulted in stable  $2n+3$  radicals on reductions. The geometries of these 11-vertex radical monoanions had, perhaps surprisingly, not been determined using computations since. A computational investigation on these systems was mentioned in the article but this study had not appeared in the literature.

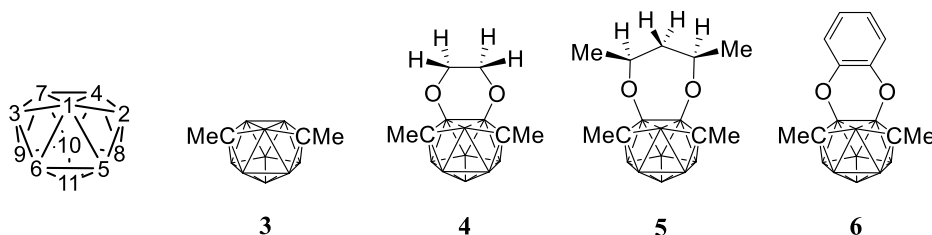


**Figure 3.** Atom numbering of the 11-vertex  $2n+2$  cluster and the 11-vertex compounds **3-6** discussed in this study.

Here we report our computational studies on carboranes **1-6** and their corresponding species on one- or two-electron reductions. The 12-vertex carboranes **1** and **2** are used as benchmarks for comparison between predicted and experimental CV and EPR data to test suitable model chemistries. These methods were then applied to 11-vertex carboranes **3-6** where we have successfully reproduced data in agreement with the observed cyclic voltammetry and electron paramagnetic resonance data available. The geometries of  $2n+3$  11-vertex radical monoanions are therefore established here for the first time.

## Results and Discussion

### 12-vertex carboranes

The cyclic voltammetry studies of the 12-vertex carboranes **1** and **2** along with their EPR spectra of their  $2n+3$  radicals shown pictorially in the literature<sup>[12,19]</sup> gave us the opportunity to compare these experimental findings with predicted energy and EPR data on **1** and **2** from various model chemistries. Computations on 1,2-diphenyl-*ortho*-carborane **1** have been explored in several studies but only one study in 2015 calculated the Gibbs free energy differences of the  $2n+3$  monoanion radical  $[\mathbf{1}]^{\cdot-}$  relative to neutral **1** and dianion  $[\mathbf{1}]^{2-}$  in the form of  $\Delta G_{\text{solv}1}$  and  $\Delta G_{\text{solv}2}$  respectively.<sup>[22]</sup> The reported model chemistry was B3LYP-GD3BJ/6-311++G(d,p) with CPCM/UKAS solvation model using acetonitrile as solvent. This computational method gave a predicted value of  $\Delta E = 400$  meV for the energy difference between the two reduction waves in **1** which is slightly higher than the observed CV value of  $\Delta E = 170$  mV for **1**.

The familiar model chemistry B3LYP/6-31G(d) with SMD solvation model using acetonitrile as solvent gave a predicted value of  $\Delta E = 180$  meV which agrees well with observed  $\Delta E = 170$  mV for **1** (Table 1). The less stable geometry of the dianion  $[\mathbf{1}]^{2-}$  reported

elsewhere<sup>[14,18,22]</sup> is used here as it is presumed to be formed initially on reduction of the monoanion radical **[1]**<sup>•-</sup> (Figure 1). Further support for the accuracy of the B3LYP/6-31G(d)/SMD(MeCN) solvation model is the good agreement between a calculated value of  $\Delta E = 580$  meV and the observed CV value of  $\Delta E = 610$  mV for **2**.

**Table 1.** Comparison of relative stabilities for the radical monoanions based on differences in solvated Gibbs free energies ( $\Delta G_{\text{solv}1}$ ,  $\Delta G_{\text{solv}2}$  and  $\Delta E$ ) in acetonitrile and observed  $\Delta E$  values from electrochemical measurements in acetonitrile.

	$\Delta G_{\text{solv}1}^{[a]}$ kcal mol <sup>-1</sup>	$\Delta G_{\text{solv}2}^{[b]}$ kcal mol <sup>-1</sup>	Computed $\Delta E^{[c]}$ meV	Observed $\Delta E^{[d]}$ mV
<b>1</b>	-72.7	-68.6	180	170
<b>2</b>	-92.4	-79.1	580	610 <sup>[e]</sup>
<b>3</b>	-73.7	-72.4	50	-
<b>4</b>	-66.0	-57.6	360	190
<b>5</b>	-65.0	-57.2	340	390
<b>6</b>	-70.5	-62.3	360	360

<sup>[a]</sup> Difference in solvated Gibbs free energies,  $\Delta G_{\text{solv}1} = \Delta G_{\text{monoanion}} - \Delta G_{\text{neutral}}$

<sup>[b]</sup> Difference in solvated Gibbs free energies,  $\Delta G_{\text{solv}2} = \Delta G_{\text{dianion}} - \Delta G_{\text{monoanion}}$

<sup>[c]</sup> Difference in computed energy,  $\Delta E = \Delta G_{\text{solv}2} - \Delta G_{\text{solv}1}$

<sup>[d]</sup> Difference in energy between two reduction half-wave potentials,  $\Delta E = E_{\text{red}1} - E_{\text{red}2}$ .

<sup>[e]</sup> In tetrahydrofuran

The calculated spin densities on **1** and **2** reveal that the unpaired radical is largely located at the two cluster carbon atoms (Table 2) with ca 53% contributions to the overall spin densities. These findings differ from the assumption that the unpaired electron is delocalized within the C<sub>2</sub>B<sub>10</sub> cluster based on the SOMO of [1]<sup>•-</sup> computed elsewhere.<sup>[12,14]</sup> The next atoms with significant degrees of spin density in [1]<sup>•-</sup> and [2]<sup>•-</sup> are the boron atoms (B3, B6) which are next to both cluster carbon atoms but they contribute less than 12% of the overall spin densities.

**Table 2.** Calculated highest spin densities and isotropic Fermi contact couplings (Fcc) for 12-vertex monoanion radicals  $[1]^-$  and  $[2]^-$  in tetrahydrofuran.

	spin $[1]^-$	spin $[2]^-$	Fcc $[1]^-$	Fcc $[2]^-$
C1	0.276	0.257	38.45	35.48
C2	0.276	0.257	38.45	35.48
B3	0.062	0.062	7.07	6.66
B6	0.062	0.062	7.07	6.66

EPR calculations were also carried out on  $[1]^-$  and  $[2]^-$  using B3LYP/EPR-II with the SMD solvation model and tetrahydrofuran as solvent. The EPR spectra for both  $[1]^-$  and  $[2]^-$  were simulated (Figure 4) and are indeed similar to the observed EPR spectra depicted in the literature with experimental line widths of 25 G for  $[1]^-$  and 28 G for  $[2]^-$  in the solid state EPR spectra. The unpaired electron is mainly located at the cluster carbons with calculated Fermi coupling constants of 35.5-38.5 G and with minor occupancies at the boron atoms (B3, B6) attached to both cluster carbon atoms with calculated coupling constants of around 7 G (Table 2).

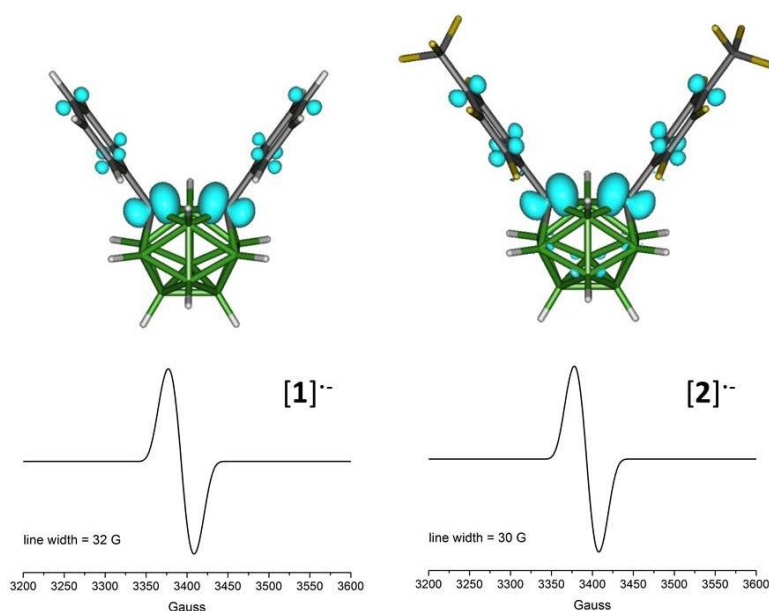


**Figure 4.** Spin density plots and simulated EPR spectra for 2n+3 monoanion radicals,  $[1]^-$  and  $[2]^-$ .

Reported<sup>[13,19]</sup> crystal structures of the neutral species, **1** and **2**, can be compared with their optimized geometries using a simple best fit method where all corresponding cluster atoms in both geometries are fitted as close as possible. The averaged misfit values for **1** and **2** are found here at 0.0108 and 0.0408 Å with the worst fit values for the cluster carbon atoms at 0.022 and 0.082 Å in **1** and **2** respectively.

### 11-vertex carboranes

For the 11-vertex carboranes discussed here, unfortunately the published<sup>[24]</sup> crystal structure data for **3** could not be obtained and no crystal structures for **4-6** are known.<sup>[25,26]</sup> The combined NMR-computational method has been shown elsewhere to be very useful in determining geometries of carboranes from observed <sup>11</sup>B NMR data.<sup>[27]</sup> Here, we confirm the ground state geometries for **3-6** shown in Figure 5 as agreement between observed<sup>[26,28]</sup> and predicted <sup>11</sup>B NMR data listed in Table 3 is excellent. While the geometry for compound **3** is expected based on the reported X-ray study<sup>[24]</sup> for **3**, the more open clusters for **4-6** contain long B1-B4 and B1-B7 distances between 2.298 and 2.365 Å. These more open geometries are reminiscent of the reported X-ray structure of 10-Br-4,7-(HO)<sub>2</sub>-2,3-C<sub>2</sub>B<sub>9</sub>H<sub>6</sub> with B1-B4 and B1-B7 distances of 2.35(2) and 2.36(3) Å.<sup>[29]</sup>

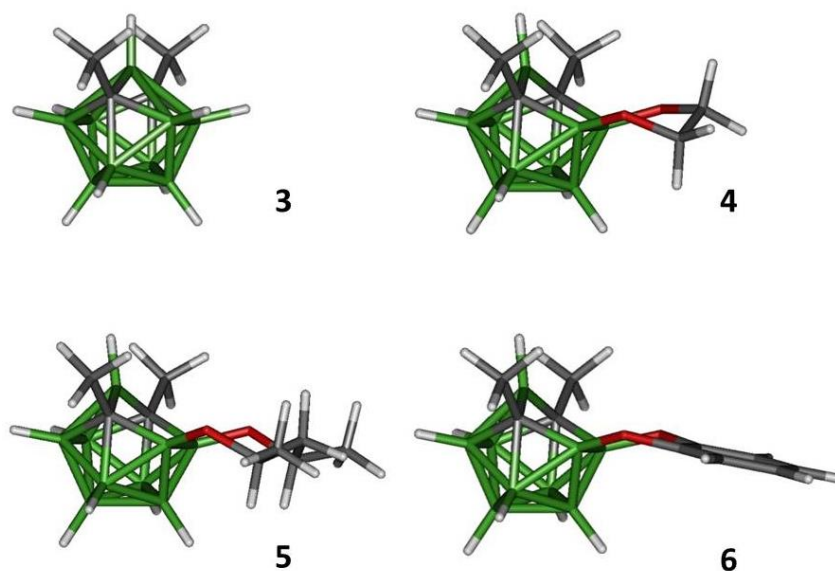


**Figure 5.** Optimized geometries for 2n+2 neutral species **3-6**.

**Table 3.** Comparison of observed and computed  $^{11}\text{B}$  NMR chemical shifts in ppm for 11-vertex carboranes **3-6** in dichloromethane.

		B4,7	B1	B8,9	B11	B5,6	B10
<b>3</b>	obs <sup>[28]</sup>	-2.9	-11.0	-6.8	-10.5	-2.9	-10.5
	calc	-3.3	-12.2	-6.3	-10.9	-3.3	-10.9
<b>4</b>	obs <sup>[28]</sup>	16.3	-1.8	-4.2	-11.6	-23.1	-23.1
	calc	15.9	-1.3	-2.9	-11.9	-22.0	-22.6
<b>5</b>	obs <sup>[26]</sup>	19.6	-0.5	-3.2	-11.8	-23.0	-26.2
	calc	19.8	0.6	-1.5	-12.3	-21.6	-25.6
<b>6</b>	obs <sup>[28]</sup>	14.5	-0.3	-4.7	-11.1	-21.5	-21.5
	calc	14.1	0.8	-2.9	-10.9	-19.7	-21.0

Compound **5** has many possible conformers with the methyl groups either *cis* or *trans* to each other and the facile flipping of the O-CHMeCH<sub>2</sub>CHMe-O bridge would take place in solution (Figure S1). If the *cis*-form is adopted it can exist as two distinct diastereoisomers with both methyl groups next to or away from the B1 atom. Modelling this particular carborane correctly is difficult as the conformer in **5** has not been established experimentally and accurate predictions are hampered by the likely facile bridge flipping processes present in solution.

Calculated spin densities on the 2n+3 monoanion radicals [**3-6**]<sup>-</sup> reveal that the unpaired electron is largely located at the three cluster boron atoms situated on the open faces (Table 4) with ca 58-75% contributions to the overall spin densities. EPR calculations were also carried out on these radicals using B3LYP/EPR-II with the SMD solvation model and tetrahydrofuran as solvent. The EPR spectra for the 11-vertex 2n+3 radicals [**3-6**]<sup>-</sup> were simulated (Figures 6 and S2) using the calculated Fermi coupling constants listed in Table 4. The simulated EPR spectrum pattern for [**6**]<sup>-</sup> with a line width of 22.2 G is remarkably similar to the observed EPR spectra depicted with the experimental line width of 22.5 G for [**6**]<sup>-</sup> in the literature.<sup>[23]</sup> The observed EPR spectra for the three 11-vertex radicals [**3-5**]<sup>-</sup> were not shown pictorially but described to be similar to [**6**]<sup>-</sup> with 10 broad lines and line width of 25 G in agreement with our simulated spectra (Figure S2).

**Table 4.** Calculated highest spin densities and isotropic Fermi contact couplings for 11-vertex monoanion radicals  $[3-6]^{-\bullet}$  in tetrahydrofuran.

	spin $[3]^{-\bullet}$	spin $[4]^{-\bullet}$	spin $[5]^{-\bullet}$	spin $[6]^{-\bullet}$	Fcc $[3]^{-\bullet}$	Fcc $[4]^{-\bullet}$	Fcc $[5]^{-\bullet}$	Fcc $[6]^{-\bullet}$
B1	0.169	0.143	0.139	0.145	23.64	22.05	20.45	20.91
B4	0.292	0.220	0.240	0.219	21.17	23.20	28.79	23.64
B7	0.292	0.252	0.240	0.219	21.17	22.03	28.79	23.64

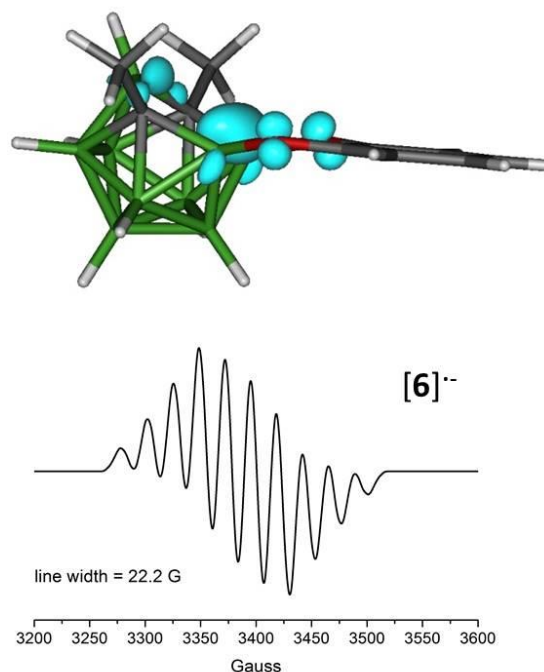


**Figure 6.** Spin density plot and simulated EPR spectrum for the 11-vertex  $2n+3$  monoanion radical  $[6]^{-\bullet}$ .

Some studies report the unusual formation of substituted 11-vertex *nido*-monoanions from deboronation-substitution of 12-vertex *closo*-carboranes with alkoxides<sup>[30,31]</sup> and fluorides.<sup>[31,32]</sup> Flipping of the BH vertex has been proposed to explain these and other 11-vertex *nido*-cluster rearrangements.<sup>[33]</sup> The fluoride ion deboronations of 1,7-(diaryl)<sub>2</sub>-*meta*-carboranes are examples of the vertex-flipping process as shown in Figure 7.<sup>[32]</sup> This process may take place via the dianion intermediate where the proton on the open face is first

removed then the BH vertex of the boron atom linked to both cluster carbon atoms is flipped and finally the proton is returned to the open face.

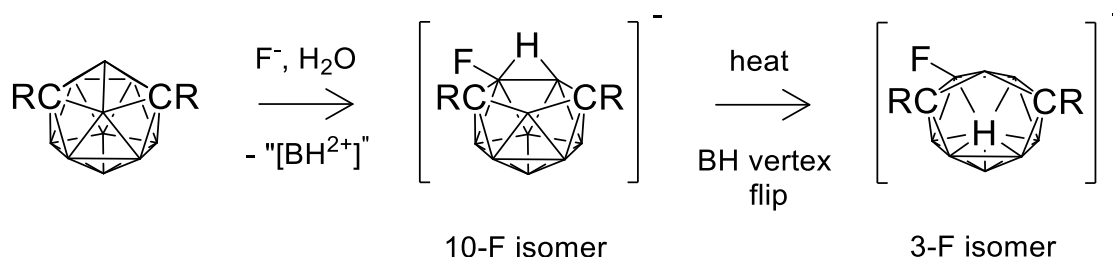


**Figure 7.** Deboronation-substitution of the 12-vertex  $2n+2$  carboranes 1,7- $\text{R}_2$ -1,7- $\text{C}_2\text{B}_{10}\text{H}_{10}$  ( $\text{R} = \text{Ph}, \text{C}_6\text{H}_4\text{F}-4'$ ) by fluoride ion to give isomeric 11-vertex  $2n+4$  carborane monoanions.

Here, the BH vertex flipping at the B1 position for **4-6** and their reduced species would give alternative geometries where the boron atoms on the open faces are not substituted. The alternative geometries of **4-6** were not located for the  $2n+2$  geometries but were found for the  $2n+3$  monoanion and  $2n+4$  dianion geometries which are denoted  $[\mathbf{4A}]^{m-}$ ,  $[\mathbf{5A}]^{m-}$  and  $[\mathbf{6A}]^{m-}$  ( $m = 1, 2$ ). The vertex-flipping transition states for the anionic species  $[\mathbf{4TS}]^{m-}$ ,  $[\mathbf{5TS}]^{m-}$  and  $[\mathbf{6TS}]^{m-}$  ( $m = 1, 2$ ) and the pathways of the vertex-flip processes were also determined. The relative energies for all these geometries are summarised in Table 5 and the six geometries for the reduced species of **4** are shown in Figure 8.

The  $2n+3$  monoanion radical geometries  $[\mathbf{4-6}]^{\cdot-}$  described earlier are more stable than the alternative geometries  $[\mathbf{4A-6A}]^{\cdot-}$ . The estimated vertex flip energy barriers are 12.7 to 14.3  $\text{kcal mol}^{-1}$  in these  $2n+3$  geometries. As the  $2n+2$  geometries **4-6** are structurally similar to the radical anions  $[\mathbf{4-6}]^{\cdot-}$ , the alternative geometries of the radicals  $[\mathbf{4A-6A}]^{\cdot-}$  are unlikely to exist in solutions kinetically as well as thermodynamically on reduction. However, the alternative  $2n+4$  dianion geometries  $[\mathbf{4A-6A}]^{2-}$  are more stable than the dianion geometries  $[\mathbf{4-6}]^{2-}$  described earlier so these results support the observed vertex flip process taking place via the dianion intermediate in some deboronation-substitution reactions of 12-vertex *closo*-carboranes with alkoxides and fluorides.<sup>[30-32]</sup> The BH flipping energy barriers in these  $2n+4$  dianions are substantial at 23.0 to 24.7  $\text{kcal mol}^{-1}$  thus severe reaction conditions (e.g. reflux) would be required for the BH flip processes to occur in the dianions of **4-6**. On this basis, alternative  $2n+4$  dianions  $[\mathbf{4A-6A}]^{2-}$  would not be present in the room-temperature electrochemical measurements carried out on **4-6**.

**Table 5.** Relative energies (in kcal mol<sup>-1</sup>) of 11-vertex geometries and vertex flip transition states.

	[4] <sup>m-</sup>	[5] <sup>m-</sup>	[6] <sup>m-</sup>	[4TS] <sup>m-</sup>	[5TS] <sup>m-</sup>	[6TS] <sup>m-</sup>	[4A] <sup>m-</sup>	[5A] <sup>m-</sup>	[6A] <sup>m-</sup>
m=1, 2n+3	0	0	0	12.7	14.3	13.9	4.2	8.7	5.7
m=2, 2n+4	6.1	6.0	3.4	29.6	29.0	28.1	0	0	0

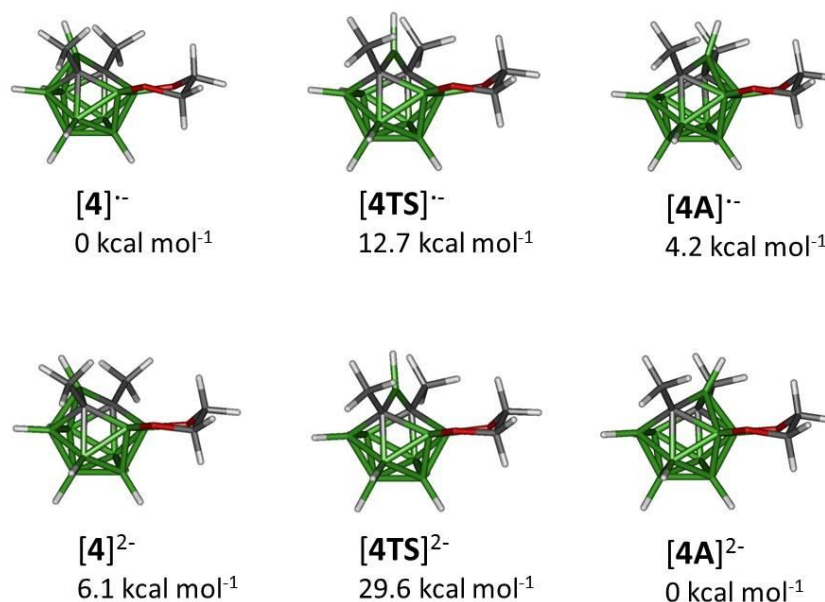


**Figure 8.** Optimized and transition state geometries for reduced species of **4** with relative energies. For animations of the vertex-flip pathways of **4** see <http://www.dur.ac.uk/m.a.fox/oliva.ppt>

### Geometry similarities

One suggestion for why 13-vertex  $2n+3$  radicals are stable was the similarity between the geometries of the neutral and radical monoanion species and a significant difference between the geometries of the radical monoanion and the dianion species.<sup>[22]</sup> Here the misfit values from the best fit method of the cluster atoms between the geometries of neutral and radical species for compounds **1-6** were obtained and are listed in Table 6. A lower misfit value reflects a better agreement between geometries. The geometries of the neutral and monoanion radical species for **4-6** are more similar than those for **1-3**. The misfit values between geometries of radical and dianion species are also included in the table for comparison. In all cases, the radical monoanion geometries are closer to the dianion geometries than to the neutral geometries. There is no correlation between the electrochemical data and the misfit

values so experimental or optimized geometries should not be used to predict whether the  $2n+3$  radical monoanions are stable.

**Table 6.** Misfit values from best fit of cluster atoms in angstroms (Å) between optimized geometries of neutral, monoanion and dianion species of **1-6** in acetonitrile.

	Averaged	Largest		Averaged	Largest
<b>1</b> vs [ <b>1</b> ] <sup>-</sup>	0.1697	0.323 (C1 or C2)	[ <b>1</b> ] <sup>-</sup> vs [ <b>1</b> ] <sup>2-</sup>	0.0772	0.146 (B3 or B6)
<b>2</b> vs [ <b>2</b> ] <sup>-</sup>	0.1563	0.293 (C1 or C2)	[ <b>2</b> ] <sup>-</sup> vs [ <b>2</b> ] <sup>2-</sup>	0.0614	0.111 (B3 or B6)
<b>3</b> vs [ <b>3</b> ] <sup>-</sup>	0.1692	0.439 (B1)	[ <b>3</b> ] <sup>-</sup> vs [ <b>3</b> ] <sup>2-</sup>	0.0671	0.112 (B1)
<b>4</b> vs [ <b>4</b> ] <sup>-</sup>	0.1034	0.214 (B1)	[ <b>4</b> ] <sup>-</sup> vs [ <b>4</b> ] <sup>2-</sup>	0.0603	0.096 (B1)
<b>5</b> vs [ <b>5</b> ] <sup>-</sup>	0.1063	0.210 (B1)	[ <b>5</b> ] <sup>-</sup> vs [ <b>5</b> ] <sup>2-</sup>	0.0628	0.094 (B10)
<b>6</b> vs [ <b>6</b> ] <sup>-</sup>	0.1041	0.236 (B1)	[ <b>6</b> ] <sup>-</sup> vs [ <b>6</b> ] <sup>2-</sup>	0.0582	0.089 (B1)

### Computational Section

All computations were carried out with the Gaussian 09 package.<sup>[34]</sup> The model geometries **1-6** and their reduced species were fully optimised with the hybrid-DFT B3LYP functional<sup>[35]</sup> with no symmetry constraints using the 6-31G(d) basis set<sup>[36]</sup> for all atoms. The SMD solvent model<sup>[37]</sup> was applied to calculations using dichloromethane (CH<sub>2</sub>Cl<sub>2</sub>), tetrahydrofuran (THF) or acetonitrile (MeCN) as solvent. Frequency calculations on these optimised geometries revealed no imaginary frequencies. The transition states were located using the QST3 method and confirmed by frequency calculations. The intrinsic reaction coordinate (irc) command was used to check the vertex-flip pathways and animations of these pathways for reduced species of **4** are found at <http://www.dur.ac.uk/m.a.fox/oliva.ppt>. The *ofit* command in the SHELXTL software package was used to obtain the misfit values between geometries.<sup>[38]</sup> Calculated <sup>11</sup>B NMR chemical shifts obtained at GIAO<sup>[39]</sup>-B3LYP/6-31G(d)//B3LYP/6-31G(d) with SMD(CH<sub>2</sub>Cl<sub>2</sub>) solvation model on the optimised geometries were referenced to BF<sub>3</sub>·OEt<sub>2</sub> for <sup>11</sup>B:  $\delta(^{11}\text{B}) = 111.7 - \sigma(^{11}\text{B})$ . Computed NMR values reported here were averaged where possible.

The spin density figures were plotted at  $\pm 0.01$  (e/bohr<sup>3</sup>)<sup>1/2</sup> with Gabedit.<sup>[40]</sup> The model chemistry B3LYP/ EPR-II<sup>[41]</sup> was used on UB3LYP/6-31G(d) optimized geometries with SMD(THF) solvation model as EPR-II is considered to be more suitable for predicting EPR

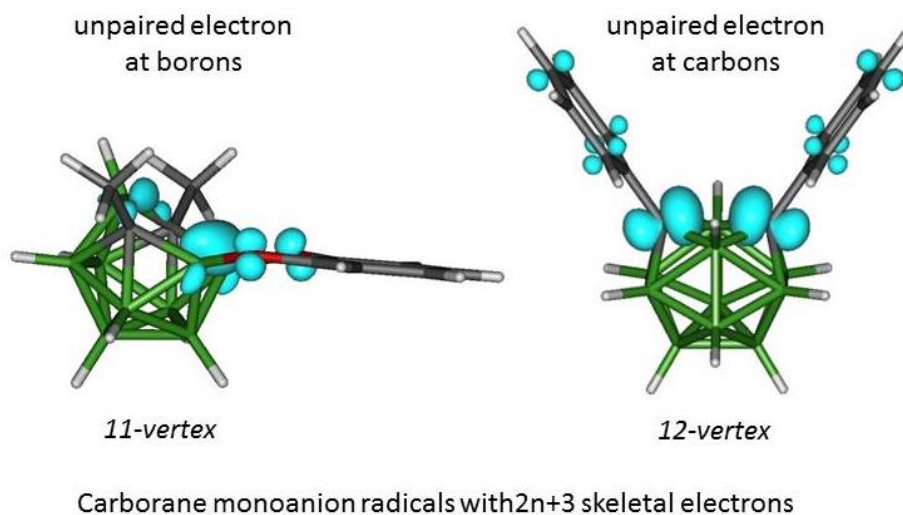
parameters. EPR simulation spectra were generated with the IsotropicRadicals program in the Biomolecular EPR Spectroscopy software suite<sup>[42]</sup> using the calculated isotropic Fermi coupling constants (FCC) and spin of 3/2 for <sup>11</sup>B nuclei along with spin of 3 and FCC at 2 Gauss to simulate <sup>10</sup>B couplings assumed to be present. There are other properties that could be predicted for carborane radical anions such as absorption,<sup>[12]</sup> infrared<sup>[12]</sup> and paramagnetic NMR<sup>[43]</sup> spectra but unfortunately such experimental data for radical anions of **3-6** have not been reported for comparison.

## Conclusions

This study demonstrates that computational methods can correctly predict electrochemical and EPR data involving 11- and 12-vertex carboranes with  $2n+3$  skeletal electron counts. Each of the geometries of the four reported 11-vertex  $2n+3$  monoanion radicals contains a  $C_2B_3$  open face. The 11-vertex  $2n+3$  geometries with tethered substituents at the open face are favored over alternative isomers where these tethered substituents are not at the open face. The unpaired electron in each 11-vertex  $2n+3$  monoanion radical is largely located over the three boron atoms on the open face. By contrast, the unpaired electron in the more common 12-vertex  $2n+3$  radical is at the cluster carbon atoms. The stability of the radical species  $2n+3$  does not appear to be strongly related to the differences between their geometries and their corresponding  $2n+2$  and  $2n+4$  geometries. The factors that make these species stable could be the high symmetries in the cluster geometries which are promoted by tethers in the case of 11- and 13- vertex carborane radical anions.

**Table of Contents entry**

Very good agreements are found between observed and simulated electron paramagnetic resonance (EPR) spectra for 11- and 12-vertex dicarbaborane radical monoanions with  $2n+3$  skeletal electrons (SE). The unpaired electron is located at the cluster borons for the 11-vertex clusters but at the cluster carbons for the 12-vertex ones.



**Keywords:** Carboranes; Skeletal electrons; Clusters; Cyclic voltammetry; Electron paramagnetic resonance

## References

- [1] R. N. Grimes, *Carboranes*, Academic Press (Elsevier), New York, 3rd edn, **2016**.
- [2] For other reviews on carboranes see
- a) V. I. Bregadze, *Chem. Rev.* **1992**, *92*, 209-223;
  - b) L. A. Leites, *Chem. Rev.* **1992**, *92*, 279-323;
  - c) J. F. Valliant, K. J. Guenther, A. S. King, P. Morel, P. Schaffer, O. O. Sogbein, K. A. Stephenson, *Coord. Chem. Rev.*, **2002**, *232*, 173-230;
  - d) T. J. Wedge, M. F. Hawthorne, *Coord. Chem. Rev.* **2003**, *240*, 111-128;
  - e) M. A. Fox, A. K. Hughes, *Coord. Chem. Rev.* **2004**, *248*, 457-476;
  - f) A. F. Armstrong, J. F. Valliant, *Dalton Trans.* **2007**, 4240-4251;
  - g) M. A. Fox, "Polyhedral Carboranes" Chapter 3.02 in *Comprehensive Organometallic Chemistry III*, Vol. 3, pp 49-112, R. H. Crabtree, D. M. P. Mingos, Elsevier, Oxford, **2007**;
  - h) V. N. Kalinin, V. A. Ol'shevskaya, *Russ. Chem. Bull.* **2008**, *57*, 815-836;
  - i) I. B. Sivaev, V. V. Bregadze, *Eur. J. Inorg. Chem.* **2009**, 1433-1450;
  - j) F. Issa, M. Kassiou, L. M. Rendina, *Chem. Rev.* **2011**, *111*, 5701-5722;
  - k) M. Scholz, E. Hey-Hawkins, *Chem. Rev.* **2011**, *111*, 7035-7062;
  - l) D. Olid, R. Núñez, C. Viñas, F. Teixidor, *Chem. Soc. Rev.* **2013**, *42*, 3318-3336;
  - m) A. M. Spokoyny, *Pure Appl. Chem.* **2013**, *85*, 903-919;
  - n) V. I. Bregadze, *Russ. Chem. Bull., Int. Ed.* **2014**, *63*, 1021-1026;
  - o) S.M. Gao, N.S. Hosmane, *Russ. Chem. Bull., Int. Ed.* **2014**, *63*, 788-810;
  - p) C. E. Housecroft, *J. Organomet. Chem.* **2015**, *798*, 218-228;
  - q) R. N. Grimes, *Dalton Trans.* **2015**, *44*, 5939-5956;
  - r) J. G. Planas, F. Teixidor, C. Viñas, *Crystals* **2016**, *6*, 50;
  - s) S. Mukherjee, P. Thilager, *Chem. Commun.* **2016**, *52*, 1070-1093;
  - t) R. Núñez, I. Romero, F. Teixidor, C. Viñas, *Chem. Soc. Rev.* **2016**, *45*, 5147-5173;
  - u) X. Li, H. Yan, Q. Zhao, *Chem. Eur. J.* **2016**, *22*, 1888-1898.
- [3] a) K.A. Bilevich, L.I. Zakharkin, O.Y. Okhlobystin, *Bull. Acad. Sci. USSR, Div. Chem. Sci.* **1965**, 1887 (Engl. Transl.); b) K.A. Bilevich, L.I. Zakharkin, O.Y. Okhlobystin, *Bull. Acad. Sci. USSR, Div. Chem. Sci.* **1967**, 435-437 (Engl. Transl.).
- [4] a) L.I. Zakharkin, V.N. Kalinin, L.S. Podvisotskaya, *Bull. Acad. Sci. USSR, Div. Chem. Sci.* **1966**, 1444 (Engl. Transl.); b) L.I. Zakharkin, V.N. Kalinin, L.S. Podvisotskaya,

- Bull. Acad. Sci. USSR, Div. Chem. Sci.* **1967**, 2212-2217 (Engl. Transl.); c) L.I. Zakharkin, *Pure Appl. Chem.* **1972**, 29, 513-526.
- [5] R. A. Harder, J. A. H. MacBride, G. P. Rivers, D. S. Yufit, A. E. Goeta, J. A. K. Howard, K. Wade, M. A. Fox, *Tetrahedron* **2014**, 70, 5182-5189.
- [6] L. Böhling, A. Brockhinke, J. Kahlert, L. Weber, R. A. Harder, D.S. Yufit, J.A.K. Howard, J.A.H. MacBride, M. A. Fox, *Eur. J. Inorg. Chem.* **2016**, 403-412.
- [7] L. I. Zakharkin, V. A. Ol'shevskaya, B. L. Tumanskii, *Metalloorganicheskaya Khimiya* **1993**, 6, 98-100 (Russ.).
- [8] a) J. H. Morris, H. J. Gysling, D. Reed, *Chem. Rev.* **1985**, 85, 51-76; b) R. Núñez, M. Tarrés, A. Ferrer-Ugalde, F. Fabrizi de Biani, F. Teixidor, *Chem. Rev.* **2016**, 116, 14307-14378.
- [9] a) B.T. King, B. C. Noll, A.J. McKinley, J. Michl, *J. Am. Chem. Soc.* 1996, **118**, 10902-10903; b) N. S. Hosmane, H. Zhang, J. A. Maguire, Y. Wang, T. Demissie, T. J. Colacort, M. B. Ezhova, K.-J. Lu, D. Zhu, T. G. Gray, S. C. Helfert, S. N. Hosmane, J. D. Collins, F. Baumann, W. Kaim, W. N. Lipscomb, *Organometallics* 2000, **19**, 497-508; c) J. Kaleta, J. Tarábek, A. Akdag, R. Pohl, J. Michl, *Inorg. Chem.* 2012, **51**, 10819-10824.
- [10] L. I. Zakharkin, V. N. Kalinin, A. P. Snyakin, *Dokl. Akad. Nauk SSSR* **1970**, 195, 1357-1360 (Russ.).
- [11] a) M. V. Yarosh, T. V. Baranova, V. L. Shirokii, A. A. Erdman, N. A. Maier, *Russ. J. Electrochem.* **1993**, 29, 789-790 (Engl. Transl.); b) M. V. Yarosh, T. V. Baranova, V. L. Shirokii, A. A. Erdman, N. A. Maier, *Russ. J. Electrochem.* **1994**, 30, 366-368 (Engl. Transl.).
- [12] M. A. Fox, C. Nervi, A. Crivello, P. J. Low, *Chem. Commun.* **2007**, 2372-2374.
- [13] M. A. Fox, C. Nervi, A. Crivello, A. S. Batsanov, J. A. K. Howard, K. Wade, P. J. Low, *J. Solid State Electrochem.* **2009**, 13, 1483-1495.
- [14] K. Hosoi, S. Inagi, T. Kubo, T. Fuchigami, *Chem. Commun.* **2011**, 47, 8632-8634.
- [15] K.R. Wee, Y.J. Cho, J.K. Song, S.O. Kang, *Angew. Chem.* **2013**, 125, 9864-9867; *Angew. Chem. Int. Ed.* **2013**, 52, 9682-9685.
- [16] G.F. Jin, J.-H. Hwang, J.-D. Lee, K.-R. Wee, I.-H. Suh, S.O. Kang, *Chem. Commun.* **2013**, 49, 9398-9400.

- [17] L. Weber, J. Kahlert, R. Brockhinke, L. Böhling, J. Halama, A. Brockhinke, H. -G. Stammler, B. Neumann, C. Nervi, R. A. Harder, M. A. Fox, *Dalton Trans.* **2013**, 42, 10982-10996.
- [18] J. Kahlert, L. Böhling, A. Brockhinke, H.-G. Stammler, B. Neumann, L.M. Rendina, P. J. Low, L. Weber, M. A. Fox, *Dalton Trans.* **2015**, 44, 9766-9781.
- [19] H. Tricas, M. Colon, D. Ellis, S. A. Macgregor, D. McKay, G. M. Rosair, A. J. Welch, I. V. Glukhov, F. Rossi, F. Laschi, P. Zanello, *Dalton Trans.* **2011**, 40, 4200-4211.
- [20] a) L. Weber, J. Kahlert, L. Böhling, A. Brockhinke, H.-G. Stammler, B. Neumann, R. A. Harder, P. J. Low, M. A. Fox, *Dalton Trans.* **2013**, 42, 2266-2281; b) S. Inagi, K. Hosoi, T. Kubo, N. Shida, T. Fuchigami, *Electrochemistry* **2013**, 81, 368-370; c) J. Kahlert, H.-G. Stammler, B. Neumann, R.A. Harder, L. Weber, M.A. Fox, *Angew. Chem.* **2014**, 126, 3776-3779; *Angew. Chem. Int. Ed.* **2014**, 53, 3702-3705.
- [21] X. Fu, H. -S. Chan, Z. Xie, *J. Am. Chem. Soc.* **2007**, 129, 8964-8965.
- [22] J. Zhang, X. Fu, Z. Lin, Z. Xie, *Inorg. Chem.* **2015**, 54, 1965-1973.
- [23] G.D. Mercer, J. Lang, R. Reed, F.R. Scholer, *Inorg. Chem.* **1975**, 14, 761-763.
- [24] C.-C. Tsai, W.E. Streib, *J. Am. Chem. Soc.* **1966**, 88, 4513.
- [25] G.D. Mercer, F.R. Scholer, *Inorg. Chem.* **1973**, 12, 2102-2107.
- [26] D. Gladkowski, F.R. Scholer, *J. Organomet. Chem.* **1975**, 85, 287-296.
- [27] a) M. Bühl, P.v.R. Schleyer, *J. Am. Chem. Soc.* **1992**, 114, 477-491; b) M. Bühl, J. Gauss, M. Hofmann, P.v.R. Schleyer, *J. Am. Chem. Soc.* **1993**, 115, 12385-12390; c) P.v.R. Schleyer, J. Gauss, M. Bühl, R. Greatrex, M. A. Fox, *J. Chem. Soc., Chem. Commun.* **1993**, 1766-1768; d) M. A. Fox, R. Greatrex, M. Hofmann, P.v.R. Schleyer, *J. Organomet. Chem.* **2000**, 614-615, 262-268.
- [28] F. R. Scholer, R. Brown, D. Gladkowski, W. F. Wright, L. J. Todd, *Inorg. Chem.* **1979**, 18, 921-924.
- [29] M. E. Leonowicz, F. R. Scholer, *Inorg. Chem.* **1980**, 19, 122-124.
- [30] W. R. Pretzer, D. A. Thompson, R. W. Rudolph, *Inorg. Chem.* **1975**, 14, 2571-2572.
- [31] A. J. Welch, A. S. Weller, *J. Chem. Soc., Dalton Trans.* **1997**, 1205-1212.
- [32] M. A. Fox, K. Wade, *Polyhedron* **1997**, 16, 2517-2525.
- [33] a) V. Chowdhry, W. R. Pretzer, D. N. Rai, R. W. Rudolph, *J. Am. Chem. Soc.* **1973**, 95, 4560-4565; b) L. J. Todd, A. R. Siedle, F. Sato, A. R. Garber, F. R. Scholer, G. D. Mercer, *Inorg. Chem.* **1975**, 14, 1249-1252; c) M. A. Fox, A. K. Hughes, J. M. Malget,

- J. Chem. Soc., Dalton Trans.* **2002**, 3505-3517; d) J. A. Ioppolo, M. Bhadbhade, M. A. Fox, L.M. Rendina, *Chem. Commun.* **2013**, 49, 3312-3314.
- [34] M. J. Frisch, G. W. Trucks, H. B. Schlegel, G. E. Scuseria, M. A. Robb, J. R. Cheeseman, G. Scalmani, V. Barone, B. Mennucci, G. A. Petersson, H. Nakatsuji, M. Caricato, X. Li, H. P. Hratchian, A. F. Izmaylov, J. Bloino, G. Zheng, J. L. Sonnenberg, M. Hada, M. Ehara, K. Toyota, R. Fukuda, J. Hasegawa, M. Ishida, T. Nakajima, Y. Honda, O. Kitao, H. Nakai, T. Vreven, Jr., J. A. Montgomery, J. E. Peralta, F. Ogliaro, M. Bearpark, J. J. Heyd, E. Brothers, K. N. Kudin, V. N. Staroverov, R. Kobayashi, J. Normand, K. Raghavachari, A. Rendell, J. C. Burant, S. S. Iyengar, J. Tomasi, M. Cossi, N. Rega, J. M. Millam, M. Klene, J. E. Knox, J. B. Cross, V. Bakken, C. Adamo, J. Jaramillo, R. Gomperts, R. E. Stratmann, O. Yazyev, A. J. Austin, R. Cammi, C. Pomelli, J. W. Ochterski, R. L. Martin, K. Morokuma, V. G. Zakrzewski, G. A. Voth, P. Salvador, J. J. Dannenberg, S. Dapprich, A. D. Daniels, O. Farkas, J. B. Foresman, J. V. Ortiz, J. Cioslowski, D. J. Fox, *Gaussian 09*, Revision A.02, Gaussian, Inc., Wallingford CT, **2009**.
- [35] (a) A. D. Becke, *J. Chem. Phys.* **1993**, 98, 5648-5652; (b) C. Lee, W. Yang, R. G. Parr, *Phys. Rev. B* **1988**, 37, 785-789.
- [36] (a) G. A. Petersson, M. A. Al-Laham, *J. Chem. Phys.* **1991**, 94, 6081-6090; (b) G. A. Petersson, A. Bennett, T. G. Tensfeldt, M. A. Al-Laham, W. A. Shirley, J. Mantzaris, *J. Chem. Phys.* **1988**, 89, 2193-2218.
- [37] A. V. Marenich, C. J. Cramer, D. G. Truhlar, *J. Phys. Chem. B*, **2009**, 113, 6378-6396.
- [38] Bruker, *SHELXTL-NT*, Version 5.1; Bruker Analytical X-ray Instruments Inc., Madison, WI, USA, **1998**.
- [39] (a) R. Ditchfield, *Mol. Phys.* **1974**, 27, 789-807; (b) C.M. Rohling, L.C. Allen, R. Ditchfield, *Chem. Phys.* **1984**, 87, 9-15; (c) K. Wolinski, J. F. Hinton, P. Pulay, *J. Am. Chem. Soc.* **1990**, 112, 8251-8260.
- [40] A. R. Allouche, *J. Comput. Chem.* **2011**, 32, 174-182.
- [41] V. Barone, *Recent Advances in Density Functional Methods*, Part I, Ed. Chong, D. P., World Scientific Publ. Co., Singapore, **1996**.
- [42] W. R. Hagen, *Visual Software Application: Isotropic Radicals*, Version 1.0; Biomolecular EPR spectroscopy CRC Press, Taylor and Francis, **2009**.
- [43] T.O. Pennanen, J. Machacek, S. Taubert, J. Vaara, D. Hnyk, *Phys. Chem. Chem. Phys.* 2010, **12**, 7018-7025.